

Research on Determination of the Reasonable Chip Breaker Geometry in Insert

Ung-Gi Ri, Kil-Song Paek & Kum-Song Ri

1Faculty of Mechanical Science and Technology, Kim Chaek University of Technology, Pyongyang 950003, Democratic People's Republic of Korea

Received: 10.09.2025 | Accepted: 24.10.2025 | Published: 06.11.2025

*Corresponding Author: Kum-Song Ri

DOI: [10.5281/zenodo.17543318](https://doi.org/10.5281/zenodo.17543318)

Abstract

Original Research Article

As the appropriate chip shape in turning affects on the surface roughness of the product, tool life, chatter and machine performance, chip breaker design is the key to form the desired chip shape. Previous researchers have studied the effect of chip breaker geometry on chip breakage and have not addressed the methodological issues of accurate geometry determination. In this paper, we determined the optimal chip breaker geometry with excellent chip breakage performance and longer tool life.

Keywords: insert; geometry; chip breaker.

Copyright © 2025 The Author(s). This is an open-access article distributed under the terms of the Creative Commons Attribution-NonCommercial 4.0 International License (CC BY-NC 4.0).

1. Introduction

Recently, many researchers have presented chip breaker design methods including analytical, empirical and numerical methods. [1,2]

Zhou et al. [3] analyzed the chip-breaking cutting condition limits using grooved cutting tools which resulted in the development of a web-based machining chip-breaking prediction system.

Yijiang et al. [4,21] presented a theoretical model for prediction of the chip curling patterns which were finally used to develop a computer-aided animation system to predict the chip flow, chip curl, and its breakability.

Ali and Murugan [5,19,20] studied how the position of chip breaker clamp and its angles can vary the chip form in oblique cutting of low carbon steels.

Gurbuz et al. [6,12,13] investigated the effect of various chip breaker geometries on cutting forces.

The chip breaker geometry is studied by Kim et al using a neural network based on the back

propagation algorithm.[7,14].

Furthermore, artificial neural networks (ANNs) were employed by Gurbuz et al. [8,15] in order to predict the effect of significant geometric elements of chip breaker such as length and angles on cutting forces in the machining of AISI 1050. Jawahir [9,17] found that a tool had an optimum performance with respect to the chip breakability and long life when chip contact length ranged 55–65 % of the natural contact length.

Patrascu and Carutasu [10,18] presented a FE model for 3D simulation of turning process with chip breaker tools.

In recent years, several studies have been carried out on finite element simulation of mild steels such as AISI 1045. The work presented by Vaziri et al. [11] developed the appropriate FE models and chose the right parameters to predict the cutting forces and chip shapes in orthogonal cutting.

The authors have been successful in studying the factors affecting on chip grinding and in analyzing

the cutting process, but they have been unable to identify trends in the effect of chip breaker geometry on chip breakage and to address the methodological issues of accurate geometry determination.

2. The determination of the reasonable chip breaker geometry in insert

2.1 The length and rake angle of land

The the land length is an important parameter that determines the tool life and chip flow.

If the the land length is larger than the contact length between the chip and the insert, the chip will not enter the chip breaker and if not, the insert will be sharpened, resulting in a decrease in the cutting force and the rigidity of the insert. Therefore, accurate determination of the land length can increase the cutting performance and prolong the tool life.

We determined the land length using the finite element analysis software DEFORM. We can calculate chip contact area and the distance between the contact points using the post-processor of DEFORM-2D because it has the function of representing the tool nodes.

Fig. 1. (a) shows the contact area between the insert and chip in the free cutting without chip breaker. From the results of DEFORM analysis, the contact length L_c between the insert and chip was 0.13 mm at the feed of 150 m/min and the depth of cut of 0.1 mm.

Fig. 1.(b) shows the contact length at the feed of 150 m/min and the depth of cut of 0.15 mm. The insert-chip contact length was measured by varying the depth of cut and the feed (Table 1).

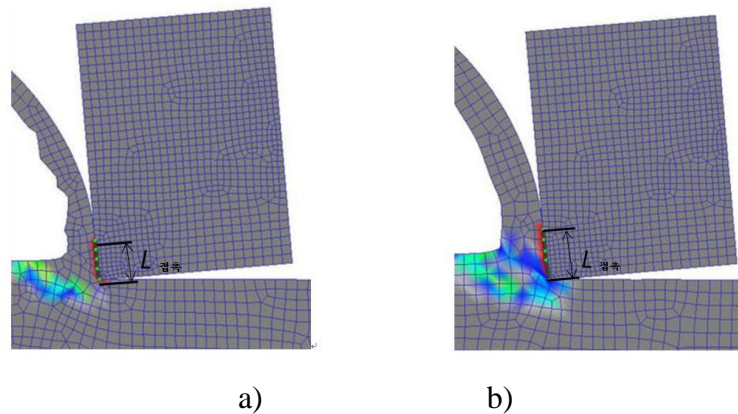


Fig.1. The contact length of the insert and chip(L_c):(a) $v=150\text{m/min}$, $a_p= 0.1\text{mm}$;
(b) $v=150\text{m/min}$, $a_p= 0.15\text{mm}$

As you can see in Table 1, the contact length shows a tendency to increase with increasing depth of cut and to increase and decrease with increasing cutting speed.

This is because the increase in depth of cut is due to the increase in rigidity of chip and the increase in resistance to deformation.

Hence, the the land length should be equal to or less than the minimum contact length.

The the land length (b_r) of the insert designed in this paper is set to be 0.14 mm with minimum contact length.

Then, the rake angle (θ_1) at the land surface was formed to ensure that the insert was safely inserted into the chip breaker.

The formation of the rake angle (θ_1) at the land surface is to reduce the cutting force under conditions of increasing the rigidity of the insert by maximizing

the land length.

In DEFORM-2D, the magnitude of the cutting force and the distribution of chip stress with and without the rake angle of the land were investigated.

Fig. 3 can be seen that the maximum stress in the case with the rake angle at the land surface is 110 MPa less than the case without the rake angle at the land surface.

When the cutting force curves with and without the rake angle at the land surface are analyzed, the difference in cutting force is about 2N, which is not significantly different. (Fig.4)

Therefore, we have chosen the corner band rake angle $\theta_1=3^\circ$. This is because the analysis of the stress shows a tendency to increase the stress rapidly at the insert from 3° , which may shorten the tool life.

Table 1. The contact length(Lc) of the insert and chip

cutting condition		The contact length of the insert and chip, mm
feed, m/min	depth of cut, mm	
100	0.1	0.14
	0.15	0.145
	0.2	0.152
150	0.1	0.16
	0.15	0.161
	0.2	0.168
200	0.1	0.141
	0.15	0.148
	0.2	0.151

2.2 The breadth, depth of the chip breaker and the rake angle at the breadth surface.

The breadth W_n and the depth of the chip

breaker H are another parameter that affects chip formation. Thus, the determination of the breadth and depth of the chip breaker is important in the design of the insert.

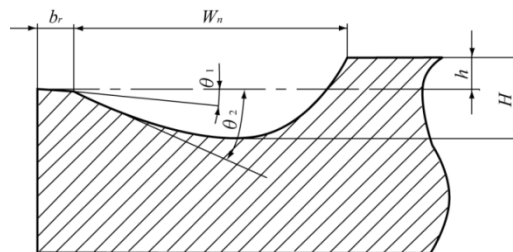


Fig.2. The geometry of the insert with chip breaker

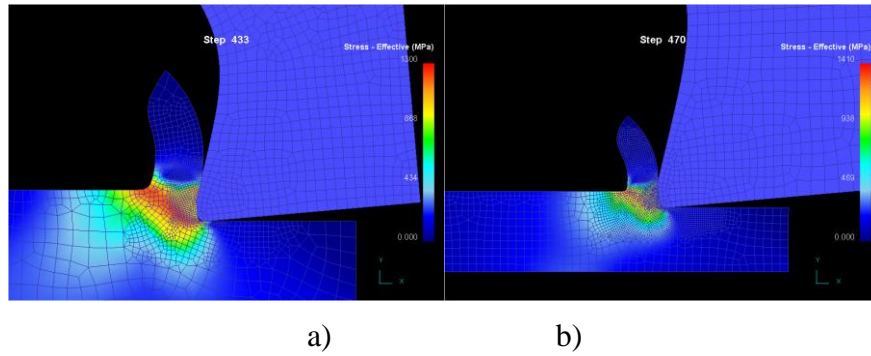


Fig. 3. The analysis of chip stress: (a). In the case with the rake angle at the land surface; (b) In the case without the rake angle at the land surface.

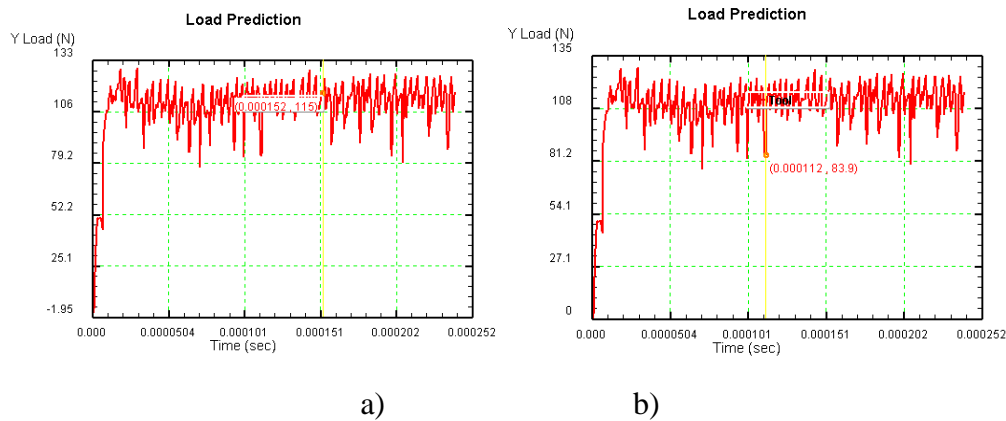


Fig. 4. The curves of the cutting force: (a). In the case with the rake angle at the land surface; (b) In the case without the rake angle at the land surface.

However, the breadth and depth of the chip breaker are not independent but correlated.

We will determine a reasonable ratio W_n/H of breadth to depth of the chip breaker.

The parameters of the tool and cutting conditions set in DEFORM were as follows (Table 2). The cutting forces were measured by changing the breadth and

depth of the chip breaker five times under the above cutting conditions.

The variation of breadth and depth of chip breaker is as follows (Table 3).

FE simulation were carried out to measure the cutting forces with the ratio W_n/H . Hence, the cutting force curves with the ratio W_n/H were obtained (Fig.5).

Table 2. The parameters of the tool and cutting conditions

inclination angle	$\lambda_0=0^\circ$
Start cutting edge angle	$k_r=45^\circ$
rake angle	$\gamma_0=-5^\circ$
depth of cut	$a_p=2.0\text{mm}$

feed	$f=0.3\text{mm/r}$
cutting speed	$v=170\text{m/min}$
material	45
difference of height between rake and flank face	$h=1\text{mm}$

As it can be seen, when $W_n/H \leq 9.5$, the main cutting force F_z increases with increasing W_n/H and then reaches a maximum value of 1914 N at $W_n/H=9.5$. This is because with increasing W_n/H , the depth of chip breaker H decreases relatively, increasing the resistance of the chip breaker to the chip, thus increasing the cutting force. When $9.5 \leq W_n/H \leq 10$, W_n/H increases, the main cutting force F_z increases and then decreases. The depth of chip breaker where the main cutting force F_z is maximum is $H=0.1\text{mm}$ and the breadth is $W_n=0.95\text{mm}$. When breadth reaches 1.0 mm, the depth becomes too small and the breadth becomes too large. Thus, the reduction of cutting force reduces the chip breakage effect.

Also, with the increase of the ratio of the breadth and depth of chip breaker, the radial force F_y is maintained at around 570N.

This indicates that it does not affect the radial force.

Also, the axial force F_x increases slightly.

Hence, a relatively small ratio should be selected to take into account the machining accuracy and surface finish.

Therefore, it is reasonable to use a ratio of W_n/H of 7.

Although the optimal determination of the ratio of W_n/H is carried out, the effect of chip breakage is different depending on how the rake angle at the breadth surface is determined at the constant ratio. It is because the rake angle at the breadth surface controls the flow of the chip, allowing the chip to flow into chip breaker and collide with the back wall, thereby affecting the chip breakage to some extent.

Therefore, a reasonable angle should be determined by measuring the chip bending moment by varying the rake angle at breadth surface γ_0 .

Table 3. The breadth and depth of chip breaker

parameters	1	2	3	4	5
breadth, mm	1.0	1.0	0.9	0.95	1.0
depth of chip breaker, mm	0.14	0.12	0.1	0.1	0.1

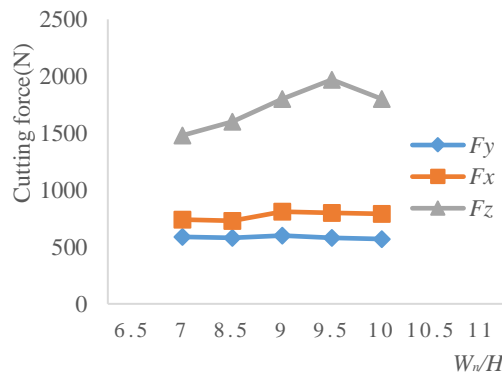


Fig. 5. The graph of the cutting force according to W_n/H

The cutting conditions in simulation are the same as those in Table 2. At constant W_n/H , the rake angle at breadth surface γ_0 must vary from 0 to 45° . This is because the insert rigidity drops sharply above 45° . At 0° , the rigidity of the insert is increased, but because of the relative increase in the cutting force and the reduction in the chip bending moment more power is consumed, so which is uneconomical in energy consumption.

As shown in Fig. 6(a), (b), in general, the bending moment increases and the cutting force also increases rapidly above 25° with increasing γ_0 .

However, for the case of γ_0 of 15° , it is reasonable to assume that the torque is large with relatively low cutting force.

Hence, the optimum rake angle at the breadth surface γ_0 is determined to be 15° .

The model of chip radius is as follows :

$$R = 2.88 \times 10^{-5} T^{-0.091} H^{-0.178} b_r^{-4.576} e^{-0.000572T} e^{0.359R} e^{23.075b_r} e^{0.188W_n} \quad (1)$$

The model of the number of turns of chip is as follows:

$$N = 0.0307 \cdot M^{0.2659} \cdot R^{1.209} \cdot e^{-0.133R} \cdot e^{0.0428W_n} \cdot e^{1.35b_r} \cdot e^{-0.251H} \quad (2)$$

N is defined as follows.

$N=0$; chip is straight.

$N=0.2$; chip is twisted;

$N=0.4$; chip is semi-rotating;

$N=0.6$; chip is a fully rotated chip;

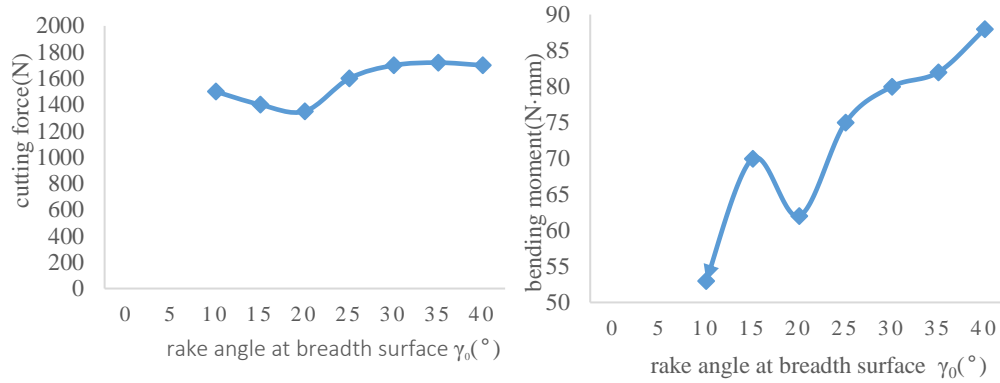
$N=0.8$; 3-9 rotations;

$N=1.0$; infinite rotation;

This model allows designers to predict chip shapes before cutting. Therefore, after the design of the inserts, the prediction of the shape of chip that can be obtained through equations [1] and [2] can be made, whereas the cutting conditions and the desired chip radius and the number of turns can be used to obtain the chip breakage groove geometry.

The chip mill groove geometry was calculated as $W_n=1.62\text{mm}$ and $H=0.23\text{mm}$ so that the number and radius of chip twist were obtained as $N=0.4$ and $R=4\text{ mm}$, respectively.

Checking whether the calculation results correspond to the reasonable ratios determined above, $W_n/H=1.62/0.23=7.04$, which is close to the reasonable ratio of 7.



a) Cutting force

b) chip bending moment

Fig.6. the cutting force and chip bending moment according to the variation of the rake angle at breadth surface

Thus, the width and depth of the obtained grinding grooves are reasonable values that are compatible with the chip grinding performance we require and reduce the power consumption by reducing the cutting force.

Based on the calculated chip breaker geometry, the insert was made.

3. The manufacturing and performance tests of the insert

3.1. The manufacturing of the insert

The die of the insert consists of a body, a stamping, a punch, and a guide pin (Fig. 7). A body is machined on spark-erosion wire cutting machine (RWC-600) and the stamping and punch are machined on CNC machine tool.

It is the most important to determine the correct contraction coefficient in manufacturing of the die.

Carbide alloy powder is used as molding powder of which composition is shown in table 3.

9.5g of powder per an insert is weighed and molded in a press at 2MPa.

Next it's sintered, aged and finally grinded. The manufactured insert is shown in Fig. 8.



Fig.7. The die of the insert

Table3. Composition of cemented carbide powders

Composition	WC	Co	TiC	TaC
Content, %	81	9	6.5	3.5

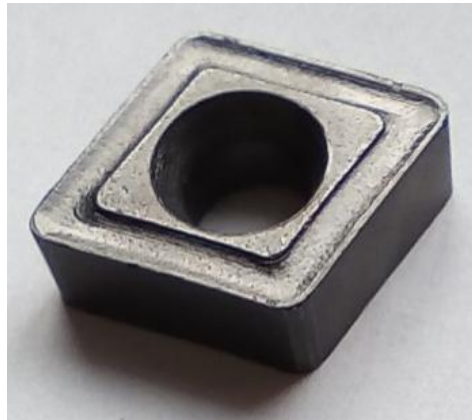


Fig. 8. The press using in molding and molded insert

3.2 Performance test

The test is carried out with the evaluation index such as chip breakability, surface finish, the tool life.

First, the chip breakability is analyzed.

The cutting conditions are as follows.

Machine tool; RT350 (CNC Lathe)

Holder: PCLNL2020K12

Cutting condition: $v=170\text{m/min}$, $ap=0.2\sim 2\text{mm}$, $f=0.1\sim 0.3\text{mm/r}$

Material: 45

Blank dimension; $\Phi 45 \times 140\text{mm}$

Cutting method: dry cutting.

Through the cutting test we can determine the suitable cutting condition.

We investigated the chip breakability of the insert by comparing the obtained chip with one published by the international process society.

We analyzed the chip breakability according to the feed rate and depth of cut when the cutting speed is constant at 170m/min . (Table 4) Fig. 9 shows various chip types obtained in the cutting test. Here, the highlight region represents the chip types with the best chip breakability where $ap \geq 1.0\text{mm}$ and $f \leq 0.15\text{mm/r}$.

Under the following conditions, we analyzed the tool life.

Material: Aisi1045

Cutting condition: $v=150\text{m/min}$, $f=0.2\text{mm/r}$, $ap=0.3\text{mm}$

Cutting method: dry cutting.

Hardness: HRC48~52

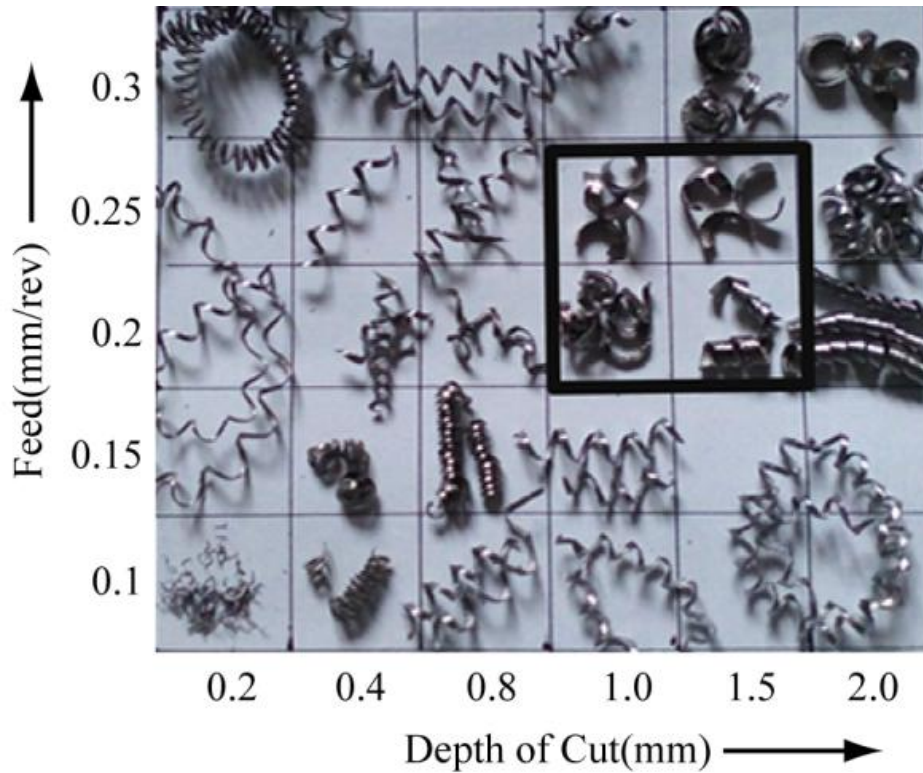


Fig. 9 Various chip types obtained in the cutting test

Table. 4. the analysis of chip breakability of insert.

Cutting condition	The types of the chip	Cause
$a_p \leq 0.2\text{mm}$, $f \leq 0.15\text{mm/r}$	Over breaking chip	The chip was cut along the workpiece surface due to too small depth of cut.
$a_p \leq 0.4\text{mm}$, $f \geq 0.15\text{mm/r}$	Continuous chip	The chip is very thin and the deformation is very small.
$a_p \geq 1.0\text{mm}$ $f \leq 0.15\text{mm/r}$	Conical helix chip	Increasing of feed rate increases chip thickness and the pressure of chip on the front surface is very large. The small convex part cannot lift the chip from the rake face and the chip is completely lifted and crushed by colliding with the back of the groove.
$a_p \geq 1.0\text{mm}$ $0.25 \leq f \leq 0.15\text{mm/r}$	Best-breaking; c-type chip	The small convex part of the tool tip increased the lateral twist of the chip.
$2 \geq a_p \geq 1.5\text{mm}$ $3 \geq f \geq 0.25\text{mm/r}$	Over breaking chip	With the increase of depth of cut and feed rate, the impact of the chip breake wall is enhanced and the breaking takes place for a certain period of time.

Table 5. performance comparison of conventional tool and the improved tool.

item Tool	Machining time per one workpiece. (min)	Number of workpiece (a unit)
Conventional cemented carbide tool	4	140
New cemented carbide tool	4	180

When the workpiece is machining with improved tools, the tool life is more than 1.3 times longer than the conventional tool.

4. Conclusion

In this paper, we determined the geometry of insert with good chip breakability and long tool life, manufactured the insert and analyzed the performance and tool life.

The land length is an important parameter that determines the tool life and chip flow, so its rake angle plays an important role in reducing the cutting force under conditions of increasing its width and increasing the rigidity of the insert.

First, we designed a new insert using mathematical model of turn and radius of chip and simulation by DEFORM. The optimum land length of 0.14 mm and the rake angle of 3° are determined through analysis using DEFORM. The depth and height of the chip breaker, their ratio and the guide angle have a great influence on the chip breakability. In this paper, through analysis using DEFORM the ratio of depth and height of chip breaker and guide angle are determined as 7 and 15°. Using the mathematical model for designing the chip breaker, we calculated its size as $W_n = 1.62$ mm and $H = 0.23$ mm, and the turns and radius of the chip as $N = 0.4$ and $R = 4$ mm.

Second, we manufactured the insert and analyzed chip breakability and tool life. The results proved that the newly designed insert has the better performance and tool life than the previous one in turning.

Acknowledgment

I would like to take the opportunity to express my heartfelt gratitude to all those who make a

contribution to the completion of my article.

Conflict of interest

The authors declare that there is no conflict of interest regarding the publication of this paper.

Disclosure statement

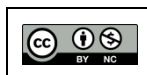
No potential conflict of interest was reported by the authors.

Data Availability

The data that support the findings of this study are available within the article.

REFERENCES

1. Qibiao Y, Zhanqiang L, Bing W (2012) Characterization of chip formation during machining 1045 steel. Int J Adv Manuf Technol 63:881–886
2. Pereira RBD, Braga DU, Nevez FO, da Silva ASC (2013) Analysis of surface roughness and cutting force when turning AISI 1045 steel with grooved tools through Scott–Knott method. Int J Adv Manuf Technol 69:1431–1441
3. Li Z, Rong YM, Li ZJ (2003) Development of web-based machining chip breaking prediction systems. Int J Adv Manuf Technol 22:336–343
4. Yijiang F (1998) Theoretical modelling and animation of the chip curling process in 3D metal cutting. University of Wollongong, Australia
5. Ali JM, Murugan M (2009) Influence of chip breaker location and angle on chip form in turning low carbon steel. Int J Mach Mach Mater 5:452–475
6. Gurbuz H, Kurt A, Korkut I, Seker U (2007) The experimental investigation of the effects of different



chip breaker forms on the cutting forces. *Adv Mater Res* 23:191–194

7. Gurbuz H, Kurt A, Seker U (2012) Investigation of the effects of different chip breaker forms on the cutting forces using artificial neural networks. *GU J Sci* 25:803–814

8. Jawahir IS (1990) On the controllability of chip breaking cycles and modes in metal cutting. *Ann ICRP* 39:47–51

9. Patrascu G, Carutasu G (2007) Using virtual manufacturing simulation in 3D cutting forces prediction. *Annals of the ORADEA University* 5:1423–1426

10. Vaziri MR, Salimi M, Mashayekhi M (2011) Evaluation of chip formation simulation models for material separation in the presence of damage models. *Simul Model Pract Theory* 19(2):718–733

11. Ozel T (2006) The influence of friction models on finite element simulations of machining. *Int J Mach Tools Manuf* 46:518–530

12. Özel T, Zeren E (2005) Finite element method simulation of machining of AISI 1045 steel with around edge cutting tool. *Int. Workshop on Modeling of Machining* soe.rutgers.edu

13. Duan CZ, Dou T, Cai YJ, Li YY (2011) Finite element simulation and experiment of chip formation process during high speed machining of AISI 1045

hardened steel. *Int. J. on Production and Industrial Engineering* June: Vol. 02, No. 01

14. Jaspers SPFC, Dautzenberg JH (2002) Material behavior in conditions similar to metal cutting: flow stress in the primary shear zone. *J Mater Process Technol* 122:322–330

15. Cockroft MG, Latham DJ (1968) Ductility and workability of metals. *J Inst Met* 96:33–39

16. Ceretti E, Lucchi M, Altan T (1999) FEM simulation of orthogonal cutting: serrated chip formation. *J Mater Process Technol* 95:17–26

17. Sowerby R, Chandrasekaran N (1984) The cold upsetting and free surface ductility of some commercial steels. *J Appl Metalwork* 3(3):257–263

18. Hua J, Shivpuri R (2004) Prediction of chip morphology and segmentation during the machining of titanium alloys. *J Mater Process Technol* 150:124–133

19. CIRP (2004) *Dictionary of production engineering*, vol 2. Springer, Berlin

20. Fang N, Jawahir IS (2002) Analytical predictions and experimental validation of cutting force ratio, chip thickness, and chip back-flow angle in restricted contact machining using the universal slip-line model. *Int. J. Machine Tools & Manufacture* 681–694